Inorganica Chimica Acta, *190* (1991) 265–269

Metal–metal bonding and charge localisation in $[Ru_2X_9]^{n-}$, X = Cl or Br; *n* = 1, 2, 3, 4. A spectroelectrochemical study

Brendan J. Kennedy*
Department of Inorganic Chemistry, University of Sydney, Sydney, NSW 2006 (Australia)

Graham A. Heath and T. Jeanne Khoo
Research School of Chemistry, Australian National University, Canberra, ACT 2601 (Australia)

(Received September 4, 1991)

Abstract

A spectroelectrochemical study of $[Ru_2X_9]^{n-}$, X = Cl, Br; *n* = 1, 2, 3, 4 has been undertaken. Stable solutions of *n* = 4, 2, 1 can be formed by electrolysis at low temperatures. Analysis of the Vis–NIR spectra of the complexes indicate that the Ru^{II}–R^{III} dimers (*n* = 4) have delocalised mixed valence and that the Ru^{III}–R^{III} (*n* = 3) dimers have a strong Ru–Ru bond. The more oxidised materials do not form a Ru–Ru bond; the spectroscopic data indicates the Ru^{III}–R^{IV} dimers have localised valency.

Introduction

The structural and electronic properties of dinuclear complexes of the type $[M_2X_9]^{n-}$, M is a transition metal and X = Cl, Br, I, which have a highly symmetrical cofacial bi-octahedral arrangement with a tri-halo bridge, are of considerable historic and current interest [1–5]. Over the past decade it has been reported that the heavier transition metals Ru, Os and Ir [6–9] form such dimers, although there is a scarcity of data on these dimers compared to the well studied complexes of the earlier TM, especially Cr, Mo, W and Re. During the same period there has been a resurgence of interest in dinuclear Ru complexes containing Cl and Group V donor (N, P, As) ligands [10–15]. It is now well established that at least some of the classical ruthenium blues are mixed valence $L_3Ru^{II}Cl_3Ru^{III}L_3$ complexes of this type [16–18]. In both classes of dimers determining the existence of M–M bonding has been paramount and for the dinuclear Ru complexes, where mixed valency is common place, there has been a desire to fully delineate the factors important in controlling the extent of valence state delocalisation.

Electrochemical characterisation has become a feature of a number of recent studies of dinuclear complexes [6, 7, 10–13]. For the 'RuX$_3$Ru' complexes it is now apparent that a number of oxidation levels from $Ru^{II}Ru^{II}$ to $Ru^{IV}Ru^{IV}$ are accessible, at least in short term electrochemical studies; the stability of the various oxidation levels depends on the nature of the terminal groups so that the electronegative $[Ru_2X_9]^{n-}$ unit is expected to stabilise the highest available oxidation state. Considering these features a spectroelectrochemical study of $[Ru_2X_9]^{n-}$ has been undertaken with the aims to: (i) determine the oxidation state stability of $[Ru_2X_9]^{n-}$, and using spectroelectrochemical techniques characterise the species generated and (ii) utilise a constant ligand geometry to determine to what extent Ru–Ru bonding occurs throughout a series of oxidation state levels and where appropriate whether valence state delocalisation occurs in the present mixed valence Ru^{II}/Ru^{III} and Ru^{III}/Ru^{IV} compounds.

Experimental

Materials

$RuCl_3 \cdot xH_2O$ was supplied by Johnson Matthey and used as received. Methylene chloride was dried by distillation over P_2O_5. (TBA)BF_4 was prepared by metathesis of $[NBu_4]Cl$ (Aldrich Chemicals) with HBF_4 in CH_2Cl_2. It was recrystallised from methylene chloride/ether and vacuum dried at 70 °C for 10 h. All other chemicals were reagent grade and were used as supplied.

Potassium tri-μ-bromo-hexabromodiruthenate-(III) was prepared by the method of Fergusson and Greenaway [19].

---

*Author to whom correspondence should be addressed.

0020-1693/91/$3.50

Tetra-n-butylammonium tri-μ-bromo-hexabromo-diruthenate(III) was prepared by metathesis of $K_2Ru_2Br_9$ with an aqueous solution of $[NBu_4]Br$. The purple solid was washed with water and diethyl ether and dried *in vacuo* at 40 °C.

Tetra-n-butylammonium tri-μ-chloro-hexachloro-diruthenate(III) was prepared as described by Coombe [20]. Complexes were characterised by IR spectroscopy and elemental analysis (C, H, N, X)

Instrumentation

UV–Vis–NIR spectra were recorded with a Perkin-Elmer λ9 spectrophotometer. The sample compartment contained an optically transparent thin-layer electrode (OTTLE) cell with a home made cryostat/cell holder constructed from PTFE [21]. A critical aspect of our experimental procedure is the retention of strict isobestic points and the full recovery of the starting spectra upon reverse electrolysis. These two criteria are essential in establishing that the electrochemical process is fully reversible with no decomposition or side reactions.

Magnetic susceptibilities were recorded by Dr K. S. Murray (Monash University) using a modified Oxford Instruments Faraday balance.

Results and discussion

Cyclic voltammetry at a stationary Pt electrode in CH_2Cl_2/0.1 M $(TBA)BF_4$ at 233 K indicates that $(TBA)_3[Ru_2Cl_9]$ undergoes two fully reversible stepwise oxidations at +0.92 and +1.58 V and a quasi reversible reduction at −0.57 V versus a Ag/AgCl reference electrode. The reversibility of this latter process is extremely sensitive to solution purity. The potentials for the analogous bromo dimer are +1.36, +0.83 and −0.60 V, respectively.

Reduction of both $[Ru_2Cl_9]^{3-}$ and $[Ru_2Br_9]^{3-}$ at −60 °C in $CH_2Cl_2/TBABF_4$ leads to the formation of intense blue solutions of the $[Ru_2Cl_9]^{4-}$ and $[Ru_2Br_9]^{4-}$ ions, respectively. These 35 electron species are relatively stable below −30 °C in pure CH_2Cl_2 solutions but are rapidly solvalised at temperatures above this by adventitious nucleophiles, e.g. H_2O. The electronic spectra of the $[Ru_2X_9]^{4-}$ ions generated *in situ* using the variable temperature OTTLE cell are both dominated by two strong bands in the visible region $\approx 15\,000$ cm^{-1} and there is a much weaker NIR absorption at ≈ 5500 cm^{-1}, Fig. 1. The two visible absorptions are not due to ligand to metal charge transfer (LMCT) processes since such transitions are expected to occur at higher energies in the 35 electron species, compared with the 34 electron species.

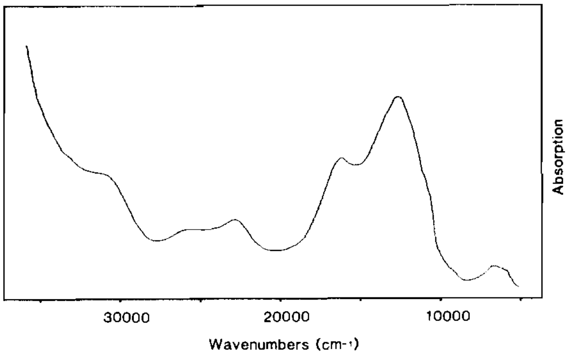

Fig. 1. Solution electronic spectrum of the electrochemically generated $(Ru_2Cl_9)^{4-}$ dimer at −60 °C. Electrolyte 0.5 M $TBA(BF_4)$ in CH_2Cl_2.

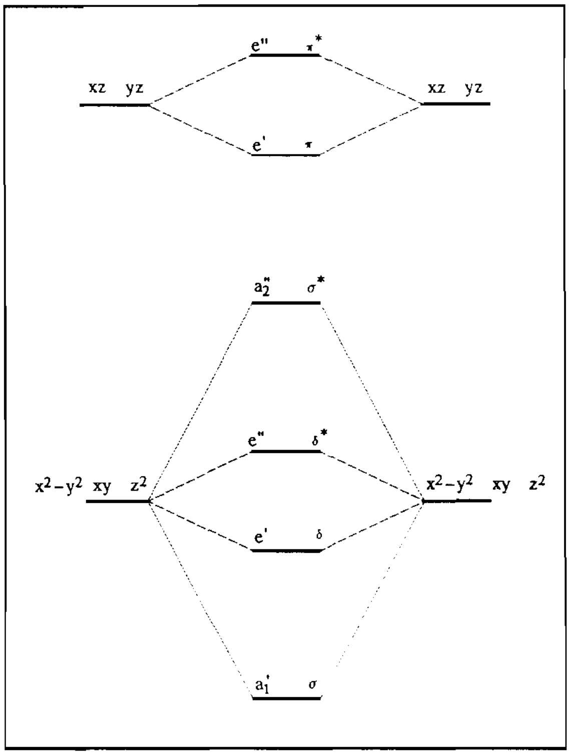

Fig. 2. Energy level diagram for combination of the d orbitals in $[Ru_2X_9]^{n-}$ in the presence of strong Ru···Ru bonding.

The electrochemical reversibility of the reduction and the ability to regenerate the starting material in 100% yield suggests that the cofacial bioctahedral geometry of the $[Ru_2X_9]$ moiety is retained. Considering the molecular orbital splitting diagram for a cofacial bioctahedron [16, 17], Fig. 2, the configuration of the ground state is $(a_1')^2(e')^4(e'')^4(a_2'')^1$. Two transitions are allowed to the singly occupied MO; a weak (*xy* polarised) transition from the e″(δ*) MO and a stronger (*z* polarised) transition from the $a_1'(\sigma)$ MO. The transition $e'(\delta) \rightarrow a_2''(\sigma^*)$ is symmetry forbidden. Consequently we believe the visible absorption band near 15 000 cm^{-1} will contain the $a_1'(\sigma) \rightarrow a_2''(\sigma^*)$ transition and we assign the weak NIR absorption to the $e''(\delta^*) \rightarrow a_2''(\sigma^*)$ transition. These assignments are the same as made for the isoelectronic $[Ru_2X_3(NH_3)_6]^{2+}$ complexes, which also have a cofacial bioctahedral geometry as confirmed by recent single crystal diffraction analysis [22, 23]. The electronic spectra of these complexes show a single intense band near 16 000 cm^{-1} and a much weaker NIR transition at ≈6500 cm^{-1}. Since it is not possible to predict a splitting of the $a_1'(\sigma) \rightarrow a_2''(\sigma^*)$ transition into two components it is probable that the second feature near 15 000 cm^{-1} is due to the $a_2''(\sigma^*) \rightarrow e''(\pi^*)$ transition, whilst the remaining strong features are ascribed to various halide to ruthenium charge transfer processes.

In the case of the stable 34 electron dimers the visible region is dominated by X→Ru CT bands, Fig. 3. However the NIR region is expected to be clear of any such absorptions and can possibly provide evidence for the approximate splitting of the 'RuX$_3$Ru' MOs. As seen in Fig. 4 the electronic spectra of $[Ru_2Cl_9]^{3-}$ at 210 K shows two relatively weak bands $\epsilon < 100$ at 5600 and 14 000 cm^{-1}. These can be assigned to the $e''(\delta^*) \rightarrow a_2''(\sigma^*)$ and $a_1'(\sigma) \rightarrow a_2''(\sigma^*)$ transitions, respectively, and the observed energies are in reasonable agreement with the values observed in the 1e reduced $[Ru_2Cl_9]^{4-}$ ion at 5900 and 12 275 cm^{-1}. For $[Ru_2Br_9]^{3-}$ the NIR spectra is somewhat less resolved but broad shoulders are observed at 5250 and ≈12 500 cm^{-1}, the latter riding on a more intense Br→Ru CT transition. These bands provide evidence supporting the presence of a delocalised MO picture for these dimers with a $S' = 0$ ground state for both ions, as postulated by Cotton and co-workers [24], and are in reasonable agreement with those calculated for solid $K_3Ru_2Cl_9$ $e''(\delta^*) \rightarrow a_2''(\sigma^*)$ 6500 and $a_1'(\sigma) \rightarrow a_2''(\sigma^*)$ 11 650 cm^{-1}. Further evidence for strong Ru–Ru bonding is provided by the relatively short Ru–Ru distances, 2.73 Å for $Cs_3Ru_2Cl_9$ [7] and 2.87 Å for $(MeEtim)_3Ru_2Br_9$ [25], and reduced room temperature magnetic moments, 0.86 and 1.18 μ_B, for the TBA salts of the chloro and bromo complexes, respectively.

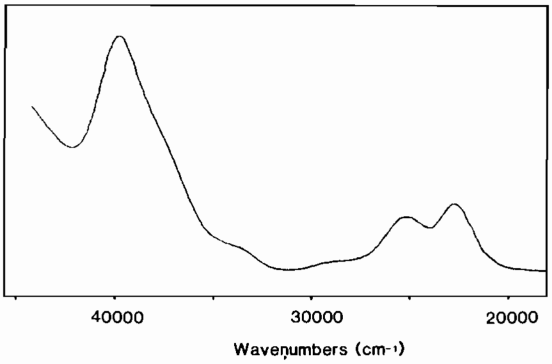

Fig. 3. Electronic spectrum of a CH_2Cl_2 solution of $(TBA)_3Ru_2Cl_9$ at 20 °C. An identical spectrum is obtained in the presence of $TBA(BF_4)$.

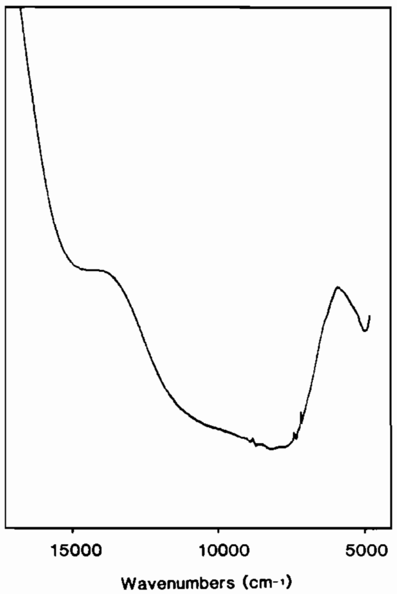

Fig. 4. NIR spectrum of a CH_2Cl_2 solution of $(TBA)_3Ru_2Cl_9$ at −60 °C.

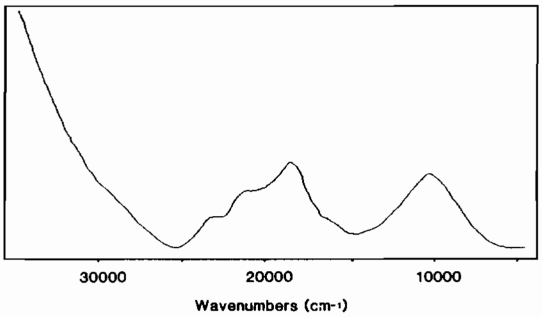

Fig. 5. Solution electronic spectrum of the electrochemically generated $(Ru_2Cl_9)^{2-}$ dimer at −60 °C. Electrolyte 0.5 M $TBA(BF_4)$ in CH_2Cl_2.

The major spectral changes observed upon 1e oxidation of $[Ru_2X_9]^{3-}$ are a decrease in the X→Ru CT transition energy of c. 4500 cm^{-1} and the growth of a moderately strong band at 10 000 cm^{-1}, Fig. 5. In the case of the bromo complex the relatively low energy of the Br→Ru CT processes results in the CT manifold occurring very close to the energy of the intense band near 10 000 cm^{-1}, which appears to be characteristic of the mixed valence Ru^{III}/Ru^{IV} state. There is little doubt that the band at 10 000 cm^{-1} is a consequence of mixed valency as it vanishes upon both the 1e oxidation and 1e reduction of

$[Ru_2X_9]^{2-}$, Fig. 6. There is no evidence for any transitions in the NIR region although, if these were weak $\epsilon < 300$, they may be obscured by intrusive electrolyte absorptions.

The extent of valence trapping in totally symmetric mixed valence dimers can be estimated by analysis of the IVCT band. Day and Mayoh [26] have shown that the extreme of $\alpha < 0.25$ corresponds to a trapped valence situation. In the present example α is calculated from the relationship $\alpha^2 = (4.24 \times 10^{-4})\epsilon(\Delta\nu_{1/2})/[d^2\nu_{max}]$ where we estimate the Ru···Ru distance, $d = 2.85$ Å, which is somewhat longer than the 2.73 Å observed for $Cs_3Ru_2Cl_9$ [7] and measure $\nu_{1/2} = 4370$, $\epsilon = 3680$ and $\nu_{max} = 10\,310$. This gives $\alpha^2 = 7.97 \times 10^2$ or $\alpha = 0.28$. For the analogous bromo dimer the Ru···Ru separation is expected to be c. 0.05–0.1 Å longer and we estimate a separation of 2.90 Å. In this case an accurate estimate of both the band halfwidth and intensity is not possible due to the strong overlap of the low energy Br → Ru CT process. Using values of $\nu_{1/2} \simeq 4300$ $\epsilon \simeq 2900$ and $\nu_{max} \simeq 1300$ we calculate $\alpha^2 = 6.76 \times 10^{-2}$ which again is indicative of a trapped valence situation.

Further evidence for a localised charged description in $[Ru_2X_9]^{2-}$ comes from the spectral changes that accompany the second 1e oxidation to the 32e dimer. The Ru_2(IV/IV) dimers are relatively unstable, and fully reversible bulk electrogeneration is only possible at low temperatures < -60 °C, and for $[Ru_2Br_9]^{1-}$ at relatively low concentrations. Even brief excursions to higher temperatures and/or trace impurities in the solvent or electrolyte, result in appreciable decomposition of the material.

Oxidation of $[Ru_2Cl_9]^{2-}$ results in the loss of the strong band at 10 000 cm^{-1}, in keeping with the assignment of the transition on to a IVCT process. More interestingly the Cl → Ru CT bands near 18 000 cm^{-1} decrease only slightly in energy to ≃17 000 cm^{-1} but they *increase* dramatically in intensity. This can be simply viewed as a consequence of increasing the number of Ru^{IV} acceptor orbitals. In addition the appearance of the higher energy portion of this spectral region appears to alter the most, presumably as a consequence of the loss of any Cl → Ru^{III} CT bands. A similar phenomena is observed for the bromo analogue, although the shift in energy of the lowest Br → Ru CT transition is very small ≃1000 cm^{-1}. The most likely assignment of the observed spectral features is that further oxidation of the localised Ru_2(III/IV) dimer produces the symmetrical Ru_2(IV/IV) dimer. A fuller analysis of the transitions is in progress and will be reported shortly.

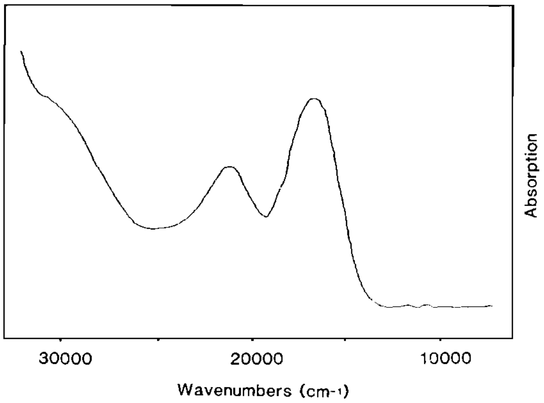

Fig. 6. Solution electronic spectrum of the electrochemically generated $(Ru_2Cl_9)^{1-}$ dimer at −70 °C. Electrolyte 0.5 M TBA(BF_4) in CH_2Cl_2.

Acknowledgement

We thank Dr K. S. Murray (Monash University) for the magnetic susceptibility measurements.

References

1 B. Briat, O. Kahn, I. Morgenstern-Badarau and J. C. Rivoal, *Inorg. Chem., 20* (1981) 4193.
2 P. J. McCarthy and H. U. Guedel, *Inorg. Chem., 23* (1984) 880.
3 B. Leuenberger, B. Briat, J. C. Canit, A. Furrer, P. Fischer and H. U. Guedel, *Inorg. Chem., 25* (1986) 2930.
4 L. Dubicki, E. Krausz, R. Stranger, P. W. Smith and Y. Tanabe, *Inorg. Chem., 26* (1987) 2247.
5 L. Dubicki and E. Krausz, *Inorg. Chem., 24* (1985) 4461.
6 V. T. Coombe, G. A. Heath, T. A. Stephenson and D. K. Vattis, *J. Chem. Soc., Dalton Trans.,* (1983) 2307.
7 J. Darriet, *Rev. Chim. Miner., 18* (1981) 27.
8 G. A. Heath and D. G. Humphrey, *J. Chem. Soc., Chem. Commun.,* (1990) 672.
9 H. J. Steinbach and W. Preetz, *Z. Anorg. Allg. Chem., 530* (1985) 155.
10 G. A. Heath, A. J. Lindsay, T. A. Stephenson and D. K. Vattis, *J. Organomet. Chem., 233* (1982) 353.
11 T. Arthur, R. Contreras, G. A. Heath, G. Hefter, A. J. Lindsay, D. J. A. Riach and T. A. Stephenson, *J. Organomet. Chem., 179* (1979) C49.
12 G. A. Heath, G. Hefter, D. R. Robertson, W. J. Sime and T. A. Stephenson, *J. Organomet. Chem., 152* (1978) C1.
13 F. A. Cotton and R. C. Torralba, *Inorg. Chem., 30* (1991) 2196.
14 F. A. Cotton, M. Matusz and R. C. Torralba, *Inorg. Chem., 28* (1989) 1516.
15 R. M. Christie, G. A. Heath, S. A. MacGregor, M. Schöder and L. J. Yellowlees, *J. Chem. Soc., Chem. Commun.,* (1990) 1445.
16 N. S. Hush, J. K. Beattie and V. M. Ellis, *Inorg. Chem., 23* (1984) 3339.

17 R. S. Armstrong, W. A. Horsfield and K. W. Nugent, *Inorg. Chem., 29* (1990) 4551.

18 K. Wieghardt, W. Hermann, M. Koppen, I. Jibrel and G. Z. Huttner, *Z. Naturforsch. Teil B, 39* (1984) 1335.

19 J. E. Fergusson and A. M. Greenaway, *Aust. J. Chem., 31* (1978) 497.

20 V. T. Coombe, *Ph.D. Thesis,* University of Edinburgh, UK, 1984.

21 C. M. Duff and G. A. Heath, *Inorg. Chem., 30* (1991) 2528.

22 J. K. Beattie, P. Del Favero, T. W. Hambley and N. S. Hush, *Inorg. Chem., 27* (1988) 2000.

23 M. N. Hughes, D. O'Reardon, R. K. Poole, M. B. Hursthouse and M. Thornton-Pett, *Polyhedron, 6* (1987) 1711.

24 B. E. Bursten, F. A. Cotton and A. Fang, *Inorg. Chem., 22* (1983) 2127.

25 D. Appleby, R. I. Crisp, P. B. Hitchcock, C. L. Hussey, T. A. Ryan, J. R. Sanders, K. R. Seddon, J. E. Turp and J. A. Zora, *J. Chem. Soc., Chem. Commun.,* (1986) 483.

26 B. Mayoh and P. Day, *J. Am. Chem. Soc., 94* (1972) 2885.